Upcycling of Waste Lithium-Cobalt-Oxide from Spent Batteries into Electrocatalysts for Hydrogen Evolution Reaction and Oxygen Reduction Reaction: A Strategy to Turn the Trash into Treasure

Seyed Ariana Mirshokraee[1], *Mohsin Muhyuddin[1], Riccardo Morina[1], Lorenzo Poggini[2], Enrico Berretti[2], Marco Bellini[2] Alessandro Lavacchi[2], Chiara Ferrara[1,3], **Carlo Santoro[1]

*e-mail: m.muhyuddin@campus.unimib.it

**e-mail: carlo.santoro@unimib.it

[1]*Department of Material Science, University of Milan Bicocca, U5 Via Cozzi 55, 20125, Milan Italy*
[2] Istituto di Chimica Dei Composti OrganoMetallici (ICCOM), Consiglio Nazionale Delle Ricerche (CNR), Via Madonna Del Piano 10, 50019 Sesto Fiorentino, Firenze, Italy
[3] National Reference Center for Electrochemical Energy Storage (GISEL), Consorzio Interuniversitario Nazionale per la Scienza e Tecnologia Dei Materiali (INSTM), via Giusti 9, Firenze, 50121, Italy

Abstract

Getting inspiration from the 'waste to resource' strategic theme of circular economy, herein, we present the upcycling of the critical raw material i.e. Co-containing waste cathode from spent lithium-ion batteries (LIBs) into platinum group metal-free (PGM-free) electrocatalysts for hydrogen evolution reaction (HER) and oxygen reduction reaction (ORR). Lithium cobalt oxide-based cathode was recovered from spent LIBs (Waste LCOd) and subsequently treated with choline chloride: citric acid 1:1 deep eutectic solvent (DES) to obtain the full degradation of the LCO-type structure and, post thermal treatments, cobalt oxide in a carbonaceous matrix (ChCl.Citric). HER and ORR activities of derived materials were investigated in alkaline media using the rotating disk electrode (RDE) and rotating ring disk electrode (RRDE), respectively. To elucidate the role of cobalt present in the derived electrocatalysts, inks were prepared by supporting the electrocatalysts with different proportions of Ketjenblack (10:90 and 50:50 ratios). Waste LCOd closely followed the electrochemical response of commercial LCO and demonstrated the least overpotential (277 mV at -10 mA cm^{-2}) for HER with an electrode configuration of 50:50. Whereas, ChCl.Citric 50:50 outperformed the other counterparts for ORR and exhibited a remarkable onset potential of 0.85 V (vs RHE) with the least peroxide production.

Keywords: oxygen reduction reaction, hydrogen evolution reaction, lithium-ion batteries, waste to resource, circular economy

1. Introduction

In the pursuit of a sustainable society, the motive of *Green Energy* is glossing under the spotlight of current research. Owing to various advantages over contemporary energy storage systems, cobalt-containing lithium-ion batteries (LIBs) are the dominating energy storage technology enabling the widespread distribution of portable electronic gadgets and of electric vehicles in the transportation sector [1]. Where the mass-scale production of LIBs outbalances the supply and demands of critical and strategic raw materials i.e. cobalt and lithium, the gigantic generation of spent batteries is provoking irrepressible complications in waste management, recycling, and reusage [2–4]. Cobalt, being largely exploited for the cathode fabrication of LIBs, has been recognized as a critical raw material because its occurrence is mainly restricted to a few geopolitically unstable regions [5]. Despite the aforementioned consideration, it is a grim reality that 30% of the worldwide production of cobalt was demanded just by the batteries industry and this figure is expected to escalate up to 53% by the year 2025 [6,7]. The scenario is becoming more challenging due to a 16.5% annual increment in the global consumption of LIB [8]. As a result, around 500 thousand tons of spent LIBs equivalent to 25 billion units were estimated to be amassed in the year 2020 [9,10]. Regardless of the enormous production of spent LIBs, a negligible focus on their viable recycling is given [11] and eventually spent LIBs have to arrive at unjustified disposal pathways i.e. landfilling, which could engender severe ecological hazards due to the presence of highly toxic metals like cobalt [12]. No doubt, several acknowledgeable endeavors for cobalt recovery from spent LIBs have been invested in the recent past [9,13–16]. However, the reusability of recycled cobalt and lithium cobalt oxide (LCO) in LIBs presents extra technology apprehensions since it is not straightforward to achieve the integrity of recovered material truly comparable to the commercial grade [17,18]. Therefore, harvesting the additional rewarding applications of recycled cobalt and LCO in a circular approach becomes extremely relevant.

In parallel, the hydrogen economy (HE) with a portfolio of green and sustainable hydrogen as an energy vector is an emerging candidate to address the predicted energy crises without contributing to the global carbon footprints. HE mainly relies on electrolyzers and fuel cells where the lethargic cathodic reactions are the key bottlenecks. Sluggish kinetics and high overpotentials of hydrogen evolution reaction (HER) and oxygen reduction reaction (ORR) at the cathode of electrolyzers and fuel cells, respectively, are typically dealt with overpriced and scarce platinum

group metals (PGMs). First raw transition metals (TM) such as Mn, Fe, Co, Ni and Cu in the form of a single atom, atomically dispersed and coordinated with nitrogen (M-N-C form), carbides, nitrides and oxides can have promising activity towards HER and ORR, especially when operating in neutral and alkaline electrolyte [19–24].

Despite being considered as a critical and strategic material, cobalt is considered one of the most potential replacements for PGMs for both HER and ORR [25–29]. Therefore, the application of LIBs recycled cobalt for HER and ORR can open an innovative window within the core of the circular economy closing the circle by reusing waste into a valuable electrochemical production and conversion system. Recently, considerable scientific interest in the waste-derived HER and ORR electrocatalysts has been witnessed where waste plastics and biomass have been deployed to fabricate advanced electrocatalysts [30–38]. A similar approach can be introduced for spent batteries considering them the cheaper source of cobalt contributing to giving waste a second life.

The recycling cost of LIBs cathodic materials can be further rationalized through the far-reaching and simplistic utilization of present TMs in electrocatalytic applications [39,40]. Not long ago, Wei et al. took an initiative to directly reuse nickel-manganese-cobalt oxides from spent LIBs for the fabrication of a bi-functional oxygen electrocatalyst which exhibited optimistic results after being applied in air batteries [41]. By the same token, Pegoretti and coworkers formulated a study to recover cobalt as $Co(OH)_2$ which was afterward utilized to produce high-temperature $LiCoO_2$ and then they evaluated its suitability for oxygen evolution reaction (OER) considering the presence of favorable Co^{3+}/Co^{4+} redox couple [42]. It is noteworthy that such a kind of structure could also be favorable for ORR if engineered properly [43,44].

At the industrial level, pyro- and hydrometallurgical processes are already implemented and allow for partial recovery of most of the heavy metals but involve high energy consumption and high environmental footprint as they exploit high temperatures above 1000°C and strong inorganic acids such as HNO_3, HCl, and H_2SO_4 that can evolve pollutants such as NO_x, SO_x [45]. For these reasons, in very recent years, new promising methods for the degradation and recycling of $LiCoO_2$ from spent LIBs have appeared in the literature [45–50]. The first option to be developed belong to the hydrometallurgical approach and involved the substitution of strong inorganic acids with organic acids such as citric, ossalic, malic in combination with reducing agents such as H_2O_2 and glucose that allow to fully degrade the $LiCoO_2$ -type cathode and, at the same time, improve the sustainability of the process as these acids are biodegradable and do not lead to the formation of

harmful gases [45-50]. In the meanwhile, this method still requires a huge amount of water due to the poor solubility of Co, Ni, Mn in an aqueous solution. Based on this, more recently the solvometallurgical approach has been proposed exploiting the Deep Eutectic Solvents (DESs), which stimulate a great interest due to the high solubility of metals in these systems, high yields of recovery, low amounts of generating waste waters, and overall high sustainability [51–53]. The choline chloride: citric acid 1:1 DES has been recently proposed as an effective leaching agent for the full degradation of $LiCoO_2$ (>99%), allowing for the recovery of >80% of cobalt [54]. Differently from this previous report, in the present study, we propose a new route for the final recovery of Co that has been performed to obtain cobalt as oxides, maintaining a carbonaceous fraction that can be beneficial for the final functional application.

In this study, commercial LCO powder purchased from Sigma Aldrich (acronym Com LCO), LCO type cathode recovered "as it is" from a spent Li-Ion battery (Waste LCOd) and LCO recovered after the recycling process based on the leaching of the Waste LCOd using the choline chloride: citric acid 1:1 DES followed by thermal treatment at 350°C to degrade the DES and obtain Co as oxide supported on carbonaceous matrix, named as ChCl.Citric were all mixed on commercial carbon black (Ketjen Black 600), characterized chemically and morphologically and tested electrochemically as HER and ORR electrocatalysts in alkaline media using the rotating disk electrode (RDE) technique.

2. Materials and Methods

2.1. Recovery of LCO from Spent Batteries

The sample labeled as Waste LCOd was recovered from a spent battery. The cylindric battery has been dismantled manually after discharge in salt water (NaCl 5 M for 24 h); the electrodes have been peeled off and the powders were removed manually after sonication in an acidic solution. The cathode powders have been characterized through XRD, SEM, EDX and thermal analysis confirming that the cathode is 93 % $LiCoO_2$ type structure while ~7 % is due to the carbon and binder content. Commercial cathode composition is not declared by the producers, and it is common to have a doping of the $LiCoO_2$ structure (LCO) with Ni and Mn (usually referred to as NMC) and/or a physical mixture of LCO and NMC. These two materials have the same structure and thus cannot be discriminated via XRD. XRF and EDX data confirm the presence of a small amount of Ni and Mn. For this reason, we referred to this sample as "Waste LCOd" to

indicate that the LCO cathode can contain doping of Ni and Mn as chemical doping or physical mixture while Co is clearly the principal metal component.

The obtained active materials have been characterized and tested without any further purification. The sample labeled as Com LCO was commercially available $LiCoO_2$ purchased from Sigma Aldrich. The sample labeled as ChCl.Citric was Waste LCOd that underwent a degradation process exploiting the choline chloride: citric acid DES. This choline chloride: citric acid DES has been prepared as previously reported [54], we here briefly recall the procedure. The choline chloride (Sigma-Aldrich) and citric acid (Sigma-Aldrich) have been mixed in a molar ratio of 1:1 in a Becker under stirring at 100°C for 2 h until the formation of a colorless liquid. The as-obtained DES has been used without any further purification for the degradation of the LCO cathode. The leaching process was performed in a climatic room at 150°C for 1 h with a rate of 100 mg of cathode vs 5 g of DES (i.e. 25 g L^{-1}) with the solution's color changing from colorless to intense blue. This solution has been dried on a hot plate at 220 °C until a viscous gel was obtained. Subsequently, the gel was treated in a muffle at 350 °C for 6 h at 10°C min^{-1} in air. The black powdered residues have been ground and washed several times with water to obtain Co in form of crystalline/amorphous oxides supported on a carbon matrix.

2.2. Materials Characterizations

Scanning Electron microscopy images were acquired with a TESCAN GAIA3 2016 dual beam equipped with a Triglav column and a field emission electron source. Images were taken at an acceleration voltage of 30 kV with the analysis mode (magnetic field-free imaging mode) using an in-chamber secondary electron detector. EDX analyses were performed with a 70 mm^2 SDD EDAX Octane Elite detector equipped with a Si_3N_4 detector. Spectra were collected at 30 kV at a working distance of 5 mm and a take-off angle of 25°. However, due to the roughness of the sample and the occurrence of large agglomerates with a tilted surface, the quantification was not pursued.

Elemental analysis was carried out using Energy-dispersive X-ray fluorescence (XRF) comprising a molybdenum anode (Bruker Artax 200 spectrometer). X-ray diffraction (XRD, Rigaku Miniflex 600) equipped with a copper source was used to perform crystallographic investigations in the 2θ range of 10-90°. To study the thermal behavior of the samples, thermogravimetric analysis (TGA) assembled with differential scanning calorimetry (DSC1, STARe system, Mettler Toledo TOLRDO) was employed. Thermal analysis was performed by

heating the sample from room temperature to 700 °C in the air at a rate of 10 °C min^{-1}. XPS experiments were carried out in a UHV chamber with a base pressure lower than 10^{-10} mbar. The chamber was equipped with non-monochromatized Al (hν=1486.6 eV) radiation and with a hemispherical electron/ion energy analyzer (VSW mounting a 16-channel detector). The operating power of the X-ray source was 120 W (12 kV and 10 mA). Photoelectrons were collected normally to the sample surface and the analyzer maintained as well the angle between the analyzer axis and the X-ray source fixed at 54.5°. All the samples were measured in fixed analyzer transmission mode with a pass energy of 44 eV. The binding energy (BE) was calibrated by setting the C1s adventitious component to 284.8 eV [55].

2.3.Electrochemical Characterizations

Electrocatalytic analyses were carried out using Pine WaveVortex RDE assembled with a Pine bipotentiostat whereas SP-100 Biologic® potentiostat was used to obtain 85% iR-compensations. The electrochemical cell, in a three-electrode arrangement, was comprised of: 1) Pt wire as a counter electrode, 2) standard calomel electrode (SCE) as a reference electrode, 3) the rotating disk electrode (RDE) and rotating ring disk electrode (RRDE) as the working electrode for HER and ORR, respectively. Eventually, all the potential values were converted to RHE by adding the factor of E_{SCE} + 0.0591 x pH to the measured potential where E_{SCE} was 0.241V.

To prepare the inks for testing, the electrocatalysts were thoroughly mixed with conductive carbon black support (Ketjenblack EC-600JD, KJ Black) in two different ratios of 10:90 and 50:50 using a mortar grinder at least for 40 min. The purpose of using two different ratios was to explicate the catalytic role of the electrocatalyst. Hence the nomenclature of electrocatalytic samples was modified with a specification of '10-90' and '50-50' to specify the ratio between the actual electrocatalysts and KJ black, respectively. Eventually, the 3 mg of the electrocatalyst-containing blend was dispersed in the mixture of 500 µl ethanol and 50 µl Nafion® D-520 ionomer solution. The suspension was then probe sonicated for 15 mins followed by bath sonication for further 45 mins at room temperature.

2.3.1. HER analysis

To examine the HER performance, the working electrode was first configured by precisely depositing the above-mentioned ink on the disk of RDE (E5 series with a disk area of 0.1963 cm^2)

using a precision pipette. After drop-casting 0.6 mg cm^{-2} loading of the electrocatalyst on the glassy carbon disk of RDE, the achieved working electrode was dried at room temperature. The HER performance was studied in nitrogen-saturated 1 M KOH solution while keeping the rotation speed of RDE at 1600 rpm. Nitrogen gas was continuously purged into the electrolyte during the whole measurement. Linear sweep voltammograms (LSVs) were acquired at 5 m Vs^{-1} after conditioning the electrocatalysts by applying multiple cyclic voltammograms (CV) at 50 m Vs^{-1} to obtain stable current values whereas the potential window was maintained between -1.05 and -2.05 V vs SCE. To analyze the working stability of the best-performing electrocatalyst, an accelerated stability test was carried out by applying potential cycling over the 2000 cycles with the scan rate of 50 mV s^{-1} and for comparison, the initial and every 500^{th} measurement was taken at the rate of 5 mV s^{-1}.

2.3.2. ORR analysis

RRDE (E6R2 series) with a disk area of 0.2376 cm^2 was employed to configure the working electrode for ORR tests with two different mass-loadings of each electrocatalyst i.e. 0.2 mg cm^{-2} and 0.6 mg cm^{-2}. The RRDE collection efficiency (N) was 38% while the area of Pt ring was 0.2356 cm^2. ORR measurements were taken in 0.1 M KOH solution by keeping the rotation speed of RRDE at 1600 rpm. The electrolytic solution was vigorously flushed with oxygen for at least 30 mins before the commencement of experimentation and then uninterruptedly bubbled throughout the measurements to guarantee an ample level of oxygen saturation. ORR potential window was investigated between 0.15 V to -1.05 V vs SCE and the ring potential was fixed at 0.15 V vs SCE. Polarization curves at 5 m Vs^{-1} were obtained after achieving a steady trend in the current values by running multiple CV cycles. Peroxide yield (%) and transformation of electrons (n) during ORR were estimated by monitoring the disk current density (I_{disk}) and ring current density (I_{disk}) according to eq.1 and eq.2, respectively.

$$Peroxide\ (\%) = \frac{200 \times \frac{I_{ring}}{N}}{I_{disk} + \frac{I_{ring}}{N}} \qquad \text{(eq.1)}$$

$$n = \frac{4\, I_{disk}}{I_{disk} + \frac{I_{ring}}{N}} \qquad \text{(eq.2)}$$

Using similar RRDE measurements, an accelerated stability test over 2000 cycles (at 50 mV s^{-1} scan rate) was performed for studying the durability attributes of the derived electrocatalyst with

optimum performance. Continuous potential cycling was carried out within the same ORR potential window in O_2 saturated 0.1 M KOH with an electrocatalyst loading of 0.6 mg cm^{-2}. The first scan and the scans after every 500 cycles were recorded at the typical rate of 5 mV s^{-1}.

3. Results and Discussion

3.1. Surface chemistry, morphology and composition characterization

3.1.2. Scanning electron microscopy images

Figure 1 shows the low magnification images of the Com LCO (a), Waste LCOd (b) and the ChCl.Citric (c). The Com LCO shows a homogeneous distribution of the particles (Figure 1 a_1-a_3) roughly in the range of 5-10 µm. A variety of shapes exist from polyhedrons to rough spheres (Figure 1 a_3). For the Waste LCOd sample, particles in the 10 µm range were found plus larger particles that may result from agglomeration with a size up to a few hundred µm (Figure 1 b_1-b_3). The ChCl. Citric sample (Figure 1 c_1-c_3) consisted mainly of large agglomerates with sizes exceeding 1 mm.

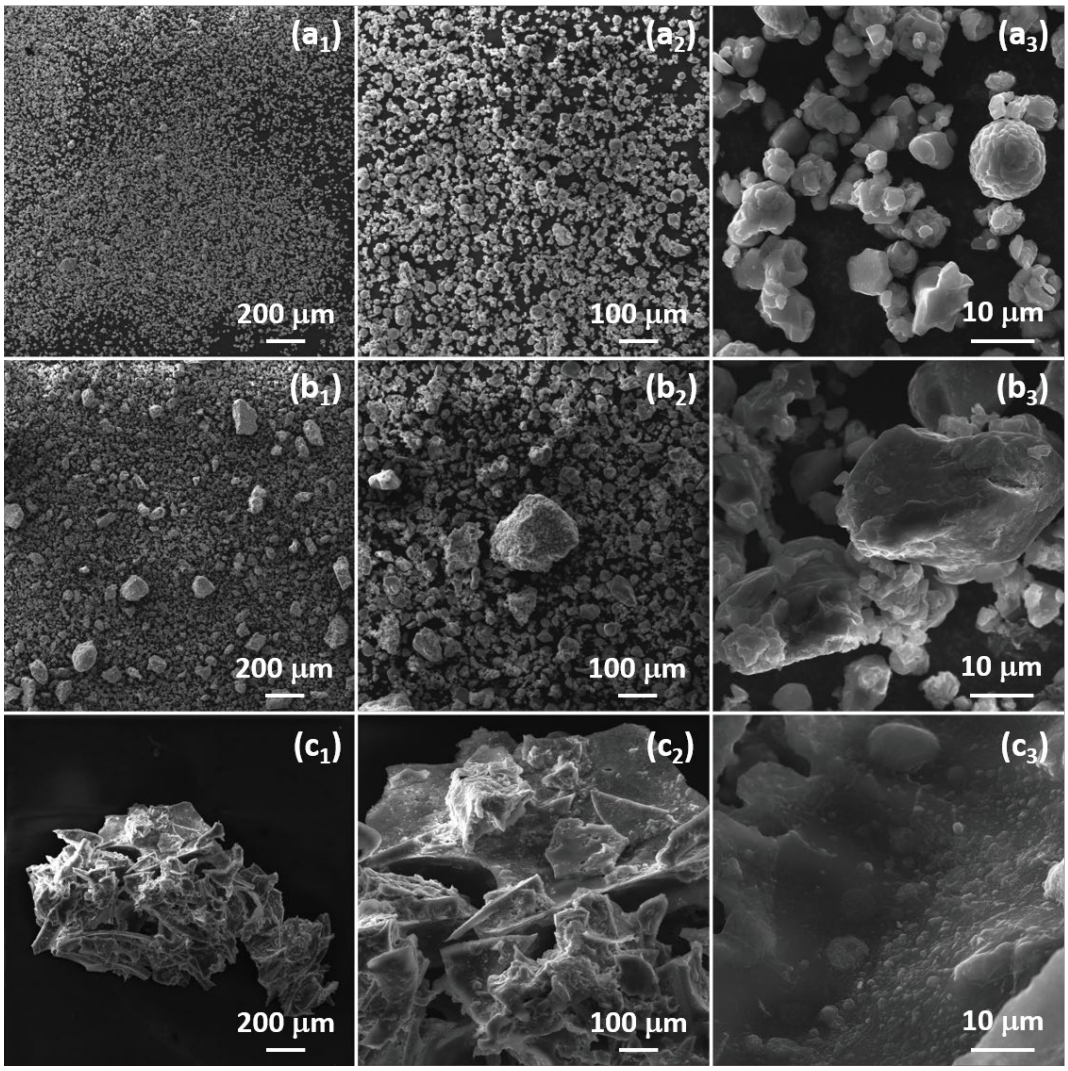

Figure 1. Secondary electron images of the samples: Com LCO (a_1-a_3), Waste LCOd (b_1-b_3) and ChCl.Citric (c_1-c_3)

The geometry of the samples did not allow a quantification of the energy-dispersive X-ray spectra due to the roughness and geometry of the samples [56,57]. However, EDX spectra show (provided in Figure S1) that the Com LCO sample only consists of Co, O and a little carbon. The waste LCO show again the occurrence of Co, O and C with the local occurrence of Ni, Mn, Si, P, S, Al, Na. In the case of the ChCl.Citric sample Co, O, Cl, N and C were found as major constituents with a limited amount of Na, F and Si and Ca traces.

3.1.3 BET, XRF and XRD analysis

The BET analysis was performed to identify the surface area. The results showed a very low surface area for all the samples and recorded to be less than 4 m^2 g^{-1}. Details are given in Supplementary Information.

With the aim of qualitative elemental analysis, XRF was utilized and achieved spectra, presented in Figure 2 a-c, categorically showed the sharp peaks of Co in all three samples whereas the traces of Ni and Mn were additionally observed in the case of Waste LCOd which are typical components of cathode material [58–60]. While the XRF of ChCl.Citric identified the presence of Co along with minor peaks of Cl. The presence of Cl can be linked with the choline chloride treatment involved in the processing of this sample. Importantly, it can be speculated that both Waste LCOd and ChCl.Citric will contain fluorine as fluorinated binders are commonly used in LIBs [61–64]. However, fluorine cannot be detected by XRF due to system limitations.

To further reveal the crystallographic details of the samples and characterize the phase composition of the considered materials, XRD was employed in the 2θ range between 10º and 90º. As can be clearly seen in Figure 2 d, the diffraction patterns of Com LCO and Waste LCOd came out to be similar as the experimental patterns are fully consistent with standard $LiCoO_2$ (JCPDS 00-050-0653)[65]. However, the XRD data for the ChCl.Citric indicates the presence of an amorphous phase with a few broad diffraction peaks that can be compatible with the presence of Co_3O_4 (JCPDS 01-080-1542) [66,67]. Indeed, the thermal treatment of the leached solution obtained after LCO degradation with DES leads to the formation of a carbonaceous matrix with an amorphous structure and promotes the formation of cobalt oxides; at the same time the low temperature involved does not allow for the full crystallization of the newly formed species thus the presence of other cobalt-based phases can be inferred. To summarize, while the Com LCO and Waste LCOd are remarkably similar as they are constituted by highly crystalline $LiCoO_2$ as the dominant phase (> 90 wt.%), the ChCl.Citric sample is significantly different as it presents a high fraction of amorphous carbon and cobalt in different species, is not fully crystallized, and cobalt is present in different oxidation states. Such hypotheses are supported by the thermal analysis results obtained for all the samples and reported in Figure S2. Indeed, the thermal profile acquired for the Com LCO indicates that no weight losses are observed in the 25-700 °C temperature range, as expected. In the same range, the Waste LCOd shows a loss of 7.63 % that has been associated with the thermal degradation of the organic binder and of the carbonaceous material present in the

electrode formulation. The ChCl.Citric on the contrary undergoes a severe thermal degradation with two steps in the 50-150 °C and 350-650 °C temperature ranges. The first one is associated with a smaller weight loss (~20 %) and imputable to the decomposition of the organic moieties of the DES while the second one is associated to the decomposition of the carbonaceous materials formed during the first step and associated with 50 % weight variation. Considering that the ChCl.Citric samples has been treated at 350 °C, it can be inferred that the carbon content of this product is in the order of 50 wt.% which is in good agreement with the XRD pattern observed for this compound.

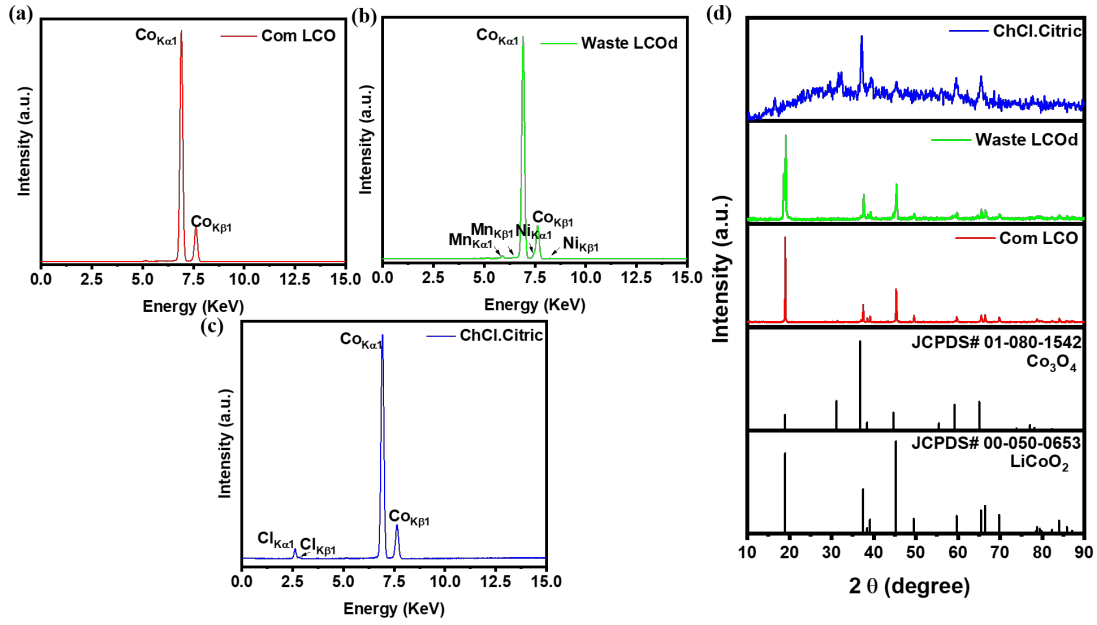

Figure 2. XRF spectra of Com LCO (a), Waste LCOd (b) and ChCl.Citric (c). XRD results of the same samples are presented in panel (d).

3.1.4 XPS analysis

XRD was employed to study the bulk crystalline structure of the samples under investigation. Also, the surface chemistry was important to be evaluated since the superficial nature of the sample may differ from the bulk material and electrochemical reactions can be affected by the surface chemistry as they take place at the surface/interface. Therefore, XPS was applied to analyze the surface chemistry of the samples and to evaluate the chemical state of Co along with a verification of the localized environment of the metal as XPS is a powerful non-

destructive technique to analyze the sample surface. The survey spectra are provided in Figure S3 while the semi-quantitative elemental analysis is provided in Table S1. The acquired data were compared with literature reference data to distinguish between different chemical states and environments [68–70]. The analyzed samples are reported in Figure 3 a-c and are compared with the reference spectra of $Co(OH)_2$, CoF_2, Co_3O_4 and CoO, respectively. As is possible to see from Figure 3 a the sample Com LCO is characterized by the same line shape as the reference spectra reported in ref. [68] with the peak of the Co 2p3/2 centered at 779.8 eV; in the other two samples, ChCl.Citric and Waste LCOd the line shape results are more complex with the peaks of the Co 2p3/2 centered at 780.5 eV and 783.4 eV, respectively. Those two samples are mostly composed of more than one chemical component; for this reason, the reference spectra [68–70] have been used as bases to obtain a reconstructed spectrum employing multiple-linear regression like reported in Figure 4 a-b to roughly estimate the composition of the sample. As a point of fact, we have to argue that this method gives us an interpretation of the composition of the system with an averaging error of the 5-10 % (obtained from the R^2 of the multiple-regression).

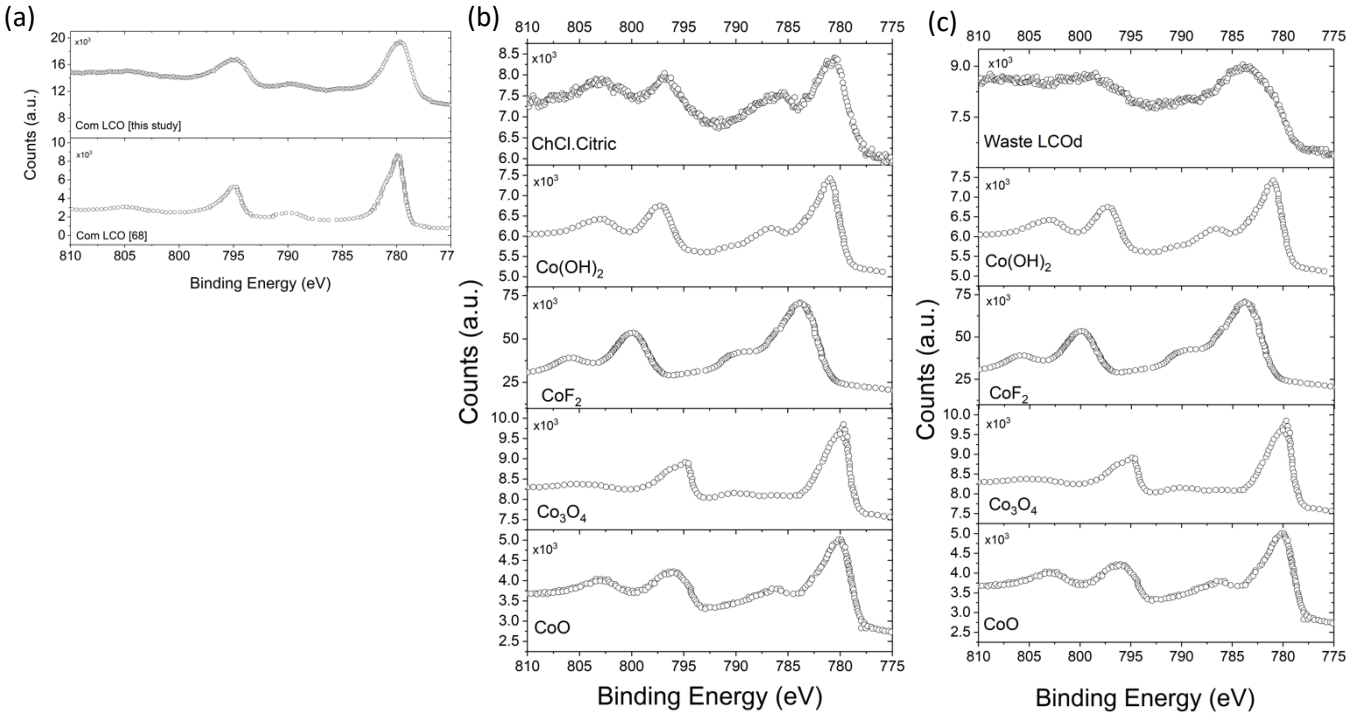

Figure 3. Experimental spectra of Com LCO (a), ChCl.Citric (b) and Waste LCOd (c) samples compared with the reference spectra.

As it is possible to see from Figure 4 a-b, all the reference components are present in the reconstructed spectra hypothesized to have a mixture of oxidation numbers of the cobalt. For the ChCl.Citric sample, the spectrum is characterized by CoO, Co_3O_4 and $Co(OH)_2$ in a ratio of ca. 6/1/2, respectively, plus a small amount of CoF_2 (less than 5 %). Indeed, for the Waste LCOd sample the composition of the reconstructed sample, results characterized by a mixture of CoF_2, CoO and $Co(OH)_2$ of ca. 50, 10 and 40 % respectively.

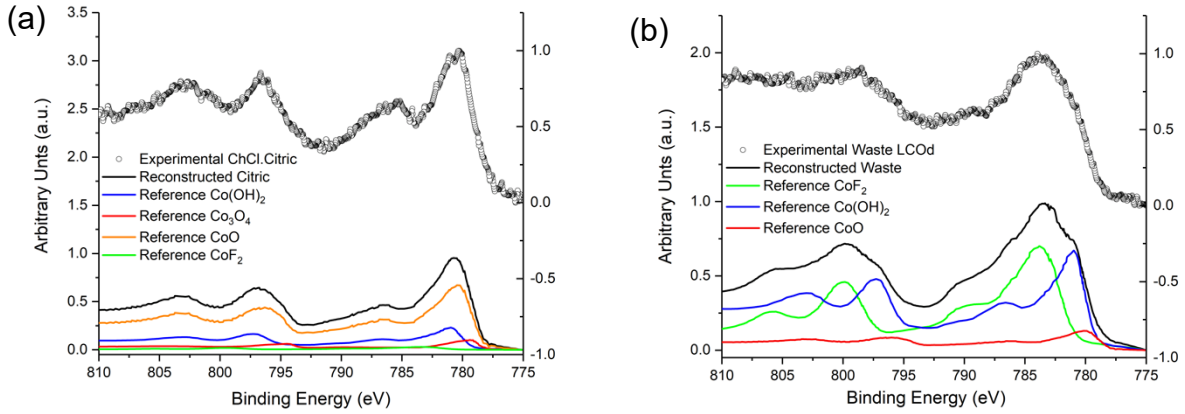

Figure 4. Experimental spectra of ChCl.Citric (a) and Waste LCOd (b) samples compared with the reconstructed spectra obtained by multiple regression.

3.2. Electrochemical results

3.2.1. HER Electrocatalysis results

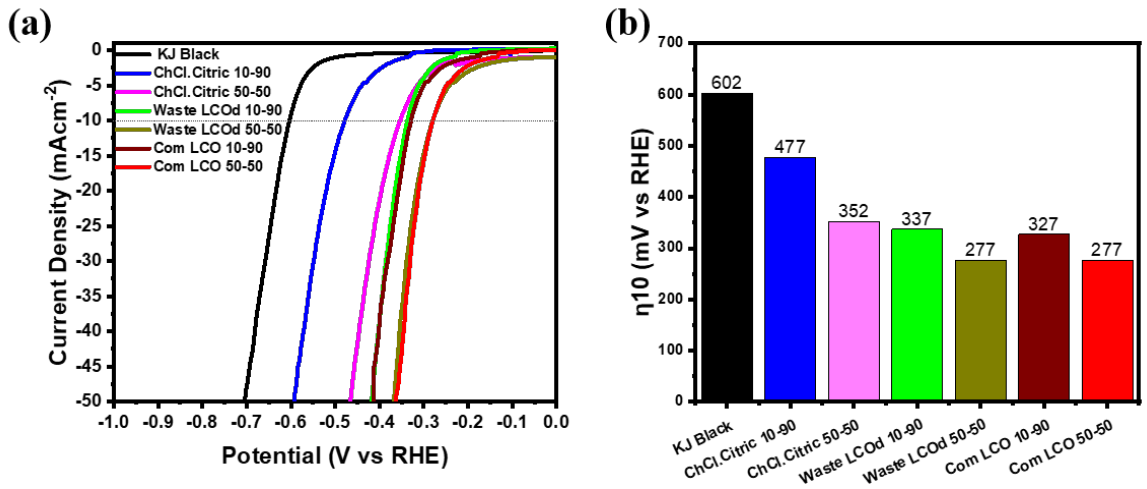

Figure 5. HER LSVs acquired at 5 m Vs^{-1} in N_2 saturated 1M KOH (a) and measured HER overpotential at 10 mA cm^{-2} (b). HER was performed with RDE while keeping the rotation speed at 1600 rpm and the acquired data are presented with 85% IR compensation. The electrode was configured with a mass loading of 0.6 mg cm^{-2} on RDE. The Co-based electrocatalysts were either supported by over 50 wt.% of carbon (50-50) or 90 wt.% of carbon (10-90).

After characterizing the LCO-based electrocatalysts, HER and ORR performance in alkaline media were investigated to identify their electrocatalytic activity and to exploit their possible suitability in anion-exchange membrane water electrolyzers (AEM-WEs) or alkaline water electrolyzers (A-WE) and anion-exchange membrane fuel cells (AEMFCs), respectively. AEM-WEs, A-WEs and AEMFCs provide an outstanding opportunity to economize the concept of HE without relying on expensive PGMs and acid-tolerant stack assembly [71,72]. However, cathodic reactions involving HER and ORR in AEM-WEs and AEMFCs, respectively, are the key bottlenecks of the given fields. Generally, the HER activity of an electrocatalyst is evaluated considering the overpotentials recorded at a current density of 10 mA cm^{-2} [73,74]. From HER polarization curves presented in Figure 5 a, it is quite evident that the pristine carbon support (KJ Black), used as control, is electrochemically inactive and imparts an exceedingly high overpotential of 602 mV (Figure 5 b). However, KJ Black was used as carbon support for the three LCO electrocatalysts to reduce the actual content of Co in the operating electrocatalysts while keeping high the electrocatalytic activity leading to a higher valorization of the waste. Moreover, it was quite complicated to prepare an ink to deposit on the glassy carbon being difficult to

homogenize the LCO within the solvent and the binder. Therefore LCO-based electrocatalysts were mixed with KJ black following two proportions of LCO to KJ black of 10-90 and 50-50. In both cases of HER and ORR electrocatalysis, increasing the relative amount of cobalt uplifted the reaction kinetics. Cathodic waste derived from spent LIBs (Waste LCOd) with KJ black ratio of 50-50, tested in terms of HER activity, presented the lowest onset potential together with a minimum overpotential (η_{10}) of 277 mV at -10 mA cm^{-2}. Notably, the HER performance of Waste LCOd without any subsequent treatment was identical to the one of commercial LCO. Interestingly, for HER, LCO subject to acid washing with citric acid (ChCl.Citric) was the less performing among the samples containing Co. Particularly, overpotential (η_{10}) of 352 mV at -10 mA cm^{-2} when was in 50-50 ratio with KJ Black and 472 mV at -10 mA cm^{-2} when was in 10-90 ratio with KJ Black (Figure 5). The leading HER performance of the Waste LCOd sample can be attributed to the presence of multiple Co-based species on the surface as confirmed by XPS and their synergic effect can be a possible reason for the least overpotential [27]. Jin and coworkers observed the collaborative effect of metallic cobalt and cobalt oxide in CoO_x@CN electrocatalysts towards HER in alkaline media [75] where cobalt oxide can be hydroxylated to dissociate water [75,76]. Similarly, Zhang et al. have also witnessed outstanding HER performance of Co/CoO_x encapsulated carbon-based electrocatalysts [77]. In addition to cobalt oxide, the efficacious role of $Co(OH)_2$ in performing HER electrocatalysis is also known [78] and interestingly this specie was also present in Waste LCOd in significant proportion. XPS further indicated the presence of a majority of Co-based moieties in the form of CoF_2 in Waste LCOd where fluorine might have by default come from the binders/additives. Interestingly, fluorine incorporation in cobalt oxide-based electrocatalysts has already been explored for the enhancement of HER performance [79]. HER performance of Waste LCOd is compared with the other Co-based electrocatalysts reported in the literature in Table S2.

In addition to a pronounced electrochemical activity, operative stability is an important merit that must be demonstrated by a capable electrocatalyst, and this factor becomes even more crucial while developing the electrocatalyst from waste products. Based on the afore-discussed leading HER performance of Waste LCOd 50-50, an accelerated HER stability test over the 2000 cycles (at the scan rate of 50 mV s^{-1}) was executed and the achieved trends are illustrated in Figure S4. Polarization curves at the beginning and after every 500 cycles were taken with a typical scan rate of 5 mV s^{-1}. A major drop in the activity was observed within the first 500 cycles where the

overpotential at -10 mA cm^{-2} increased to ~300 mV from 277 mV. Afterward, the potential degradation steadily increased along the applied cycles and eventually 43 mV increase in the overpotential was observed.

3.2.2. ORR Electrocatalysis

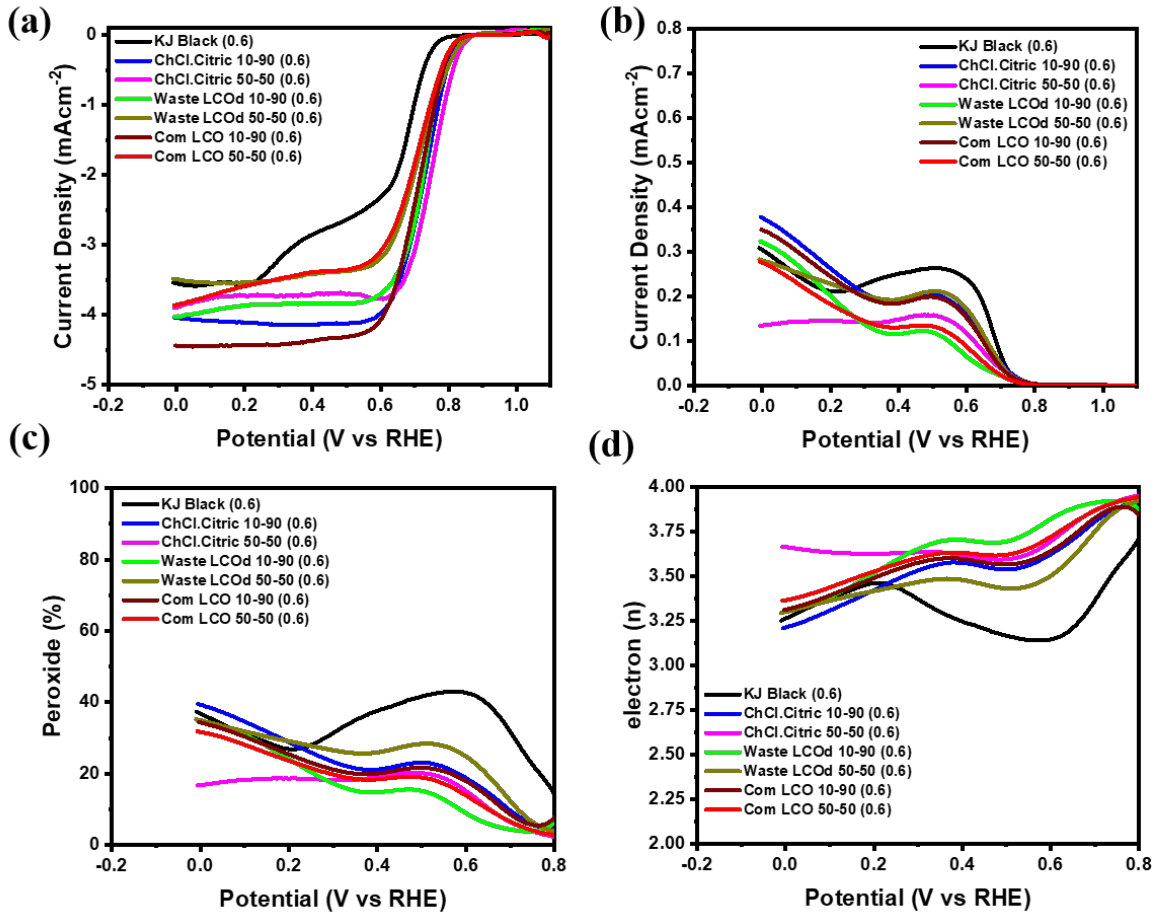

Figure 6. ORR LSVs (at the scan rate of 5 m Vs^{-1}) in O_2 saturated 0.1M KOH (a), ring current densities (b), trends of peroxide production (c) and electron transfer during ORR (f). RRDE was used to fabricate the working electrode for ORR while keeping the mass loading of 0.6 mg cm^{-2} on RRDE. The rotation speed of RRDE was maintained at 1600 rpm. Where the Co-based electrocatalysts were either supported by over 50 wt.% of carbon (50-50) or 90 wt.% of carbon (10-90).

To probe the activity of derived samples for the FCs application as ORR electrocatalysts, RRDE measurements in oxygen-rich 0.1 M KOH were executed. It is known in the community that an increase in the mass loading on the RRDE can modify the electronic pathway of oxygen electro-reduction by entrapment and subsequent reduction of undesirably produced peroxide within the thicker deposited layer [80–84]. Therefore, two different loadings of 0.2 and 0.6 mg cm^{-2} were employed in the study. ORR results with 0.2 mg cm^{-2} mass loading on RRDE are separately illustrated in supplementary Figure S5 a-d. Remarkably, all the samples came out to be electrochemically active for ORR electrocatalysts where the least activity was demonstrated by pristine KJ black, indicating the boosting of ORR kinetics primarily due to Co. Contrary to HER, the ChCl.Citric performed the best for ORR among the derived electrocatalysts as shown in Figure 6 a. Whereas ChCl.Citric 50-50 with mass loading of 0.6 mA cm^{-2} demonstrated a promising onset potential (E_{onset}) of 0.85 V (vs RHE) together with a half-wave potential ($E_{1/2}$) of 0.76 V (vs RHE) where Waste LCOd 50-50 drove the ORR with E_{onset} of 0.83 V (vs RHE) and $E_{1/2}$ of 0.7 V (vs RHE). Ring current densities (I_r) of all the samples went on increasing with a subsequent increment in the overpotential which as a result influenced the following path of ORR. However, this phenomenon got restricted to ChCl.Citric 50-50 particularly when its loading on RRDE was three-fold increased (Figure 6 b). With 0.6 mg cm^{-2} loading, ChCl.Citric 50-50 yielded peroxide maximum of up to 20% with an electron transfer number above 3.5. Moreover, Waste LCOd and commercial (Com) LCO again performed similarly, however, relatively higher peroxide production categorizes them as peroxide-producing electrocatalysts. It can be noticed that the peroxide produced increased at a higher overpotential indicating that the electrocatalysts were peroxide producers. Comparing the electrochemical performance at two different loadings (0.2 and 0.6 mg cm^{-2}), an uplift in the kinetics descriptors (i.e. $E_{1/2}$) can be noticed while a lower percentage of intermediate indicates that the peroxide is reduced within the thicker electrocatalytic layer. It is quite interesting that ChCl.Citric outperformed Waste LCOd which previously showed peak HER performance and the reason for this discrepancy could be linked with structural attributes and surface chemistry. In ChCl.Citric, where the XRD measurements confirmed the occurrence of Co_3O_4 in the matrix of amorphous/disordered carbon, XPS additionally indicates the co-presence of CoO and $Co(OH)_2$. Such an assorted structure might be helpful in uplifting the overall ORR activity. Reasonably porous-disordered carbon could be beneficial in maintaining high conductivity and mass transportation to active sites while the carbon defects are already

known for the binding of oxygen [85–89]. Moreover, both Co_3O_4 and CoO are known as PGM-free electrocatalysts with high activity, stability and robustness in alkaline conditions [28,90–93]. Inner oxygen vacancies and proportion of Co^{3+}/Co^{2+} are also relatable to the enhancement of ORR [28,94]. To compare the ORR performance of ChCl.Citric 50-50 (0.6 mg cm^{-2} loading) with previously reported Co-based electrocatalysts, Table S3 is presented in the supplementary file. The results obtained in this study show a good performance of the electrocatalyst towards ORR.

Getting motivation from the reasonably high ORR performance delivered by ChCl.Citric 50-50 with 0.6 mg cm^{-2} loading, its durability was examined over 2000 cycles while maintaining the same potential window and electrolytic conditions. However, continuous potential cycling was carried out at the scan rate of 50 mV s^{-1} whereas the initial and every 500^{th} scan was recorded at the rate of 5 mV s^{-1}. The achieved trends of accelerated stability measurements are demonstrated in Figure S6. Interestingly, ChCl. Citric 50-50 didn't show any significant decay in the E_{onset} and $E_{1/2}$ over the continuous potential cycling, however, the limiting current density tended to reduce with subsequent cycles. Similarly, the ring current density shot up as the cycles proceeded. As a linked consequence of these two effects, peroxide yield was enhanced with a corresponding decrease in electron transfer. By the end of the 2000^{th} cycle, peroxide production got nearly doubled while the number of electrons transferred dropped from 3.6 to 3.2, suggesting the alteration in the reduction mechanism involved. No doubt, the stability of the best performing electrocatalyst (ChCl. Citric 50-50) is not ideal, however, the embryonic idea of waste-derived electrocatalysts pledges revolutionary advancements within the core of the circular economy, moreover, future scientific attempts can definitely solve the durability issue in such electrocatalysts.

Perspective

The Green Revolution involving batteries and technologies of hydrogen production & conversion (i.e. electrolyzers and fuel cells) mostly rely on critical raw materials such as Co and PGMs, respectively. The scarcity and criticality of such materials jeopardize the large-scale deployment of green electrochemical technologies. In comparison with hydrogen-based systems, batteries are no doubt more commercially diffused, however, the theme of the hydrogen economy is getting worldwide acknowledgment owing to its unparalleled merits where the recycling of spent LIBs wastes could help in further boosting the evolution of hydrogen-based technologies.

The challenge of utilizing Co in LIBs can be partially alleviated by reducing its content or completely substituting Co with Ni coupled with Fe or Mn providing promising initial results [95–98]. Another practical route could be the recycling of LIBs to recover the materials of interest, mainly focusing on Co. However, as reported in the introduction, many routes have been considered sharing mainly the negative features such as high cost, utilization of many chemicals not necessarily environmentally friendly and production of hazardous side products. Moreover, the recovery of Co can reach high figures (85%) but the complete recovery remains difficult.

In parallel, the TM required in fuel cells and electrolyzers are exactly the TMs that are currently used in LIB and the TMs that are nowadays being studied to substitute Co. Therefore, the presented study outlines the possibility of direct employment of LIB cathodic waste as valuable electrocatalysts to carry out cathode side reactions in electrolyzers and fuel cells operating in alkaline environments and such strategies can help in the large deployment of these technologies at a contained cost. The change of chemistry used in the LIBs pursued to decrease the Co usage will also lead to the insertion of other elements such as Ni, Fe and Mn that could be of even greater interest for ORR and HER leading to higher electrocatalytic activity. Moreover, the recovered TMs could be also exploited in other emerging electrochemical systems such as for the carbon dioxide reduction reaction, nitrogen fixation, or nitrate reduction reaction. Future works will comprehend these directions as well as transforming and upgrading the waste LIB cathode to other chemical structures and coordination that might be more active for the reactions of interest using less impacting techniques and chemicals compared to the one nowadays used for recovering Co for reusing it in LIB

Conclusions

In a nutshell, the study underlines the prospects of valorizing the waste cathode of spent LIBs into PGM-free electrocatalysts for HER and ORR in alkaline media. Waste LCOd was recovered directly from the cathodic waste of the spent batteries and subsequently subjected to a leaching treatment in choline chloride: citric acid 1:1 DES and then heated at 350 °C to degrade the DES, giving cobalt oxide containing carbon matrix (ChCl.Citirc). As the proportion of Co-based derived electrocatalysts increased in the electrochemical inks containing KJblack as carbon support, the overall activities were enhanced drastically, indicating the sole contribution of cobalt in uplifting the reaction kinetics. Waste LCOd directly acquired from the waste cathode without

any further treatment showed electrocatalytic activities comparable to that of commercial LCO and demonstrated suitability for HER while ChCl.Citric came out to be the most active for ORR. The least HER overpotential of 277 mV at -10 mA cm^{-2} in the case of Waste LCOd 50-50 could be attributed to the synergic effect of different Co-based species as confirmed through XPS. On the other hand, cobalt-based oxides including Co_3O_4 in the matrix of amorphous/disordered carbon could be linked with the excellent ORR activity of ChCl.Citirc. With mass loading of 0.6 mg cm^{-2} on RRDE, ChCl.Citric 50-50 demonstrated an outstanding E_{onset} of 0.85 V with a nearly tetra-electronic pathway of ORR while keeping peroxide production maximum at 20%. No doubt, the electrocatalytic activities of the derived electrocatalysts are inferior compared to scarce and economically unviable PGM-based electrocatalysts but prospective endeavors could improve the electro-kinetics of the waste-derived electrocatalysts. Such approaches can give rise to new opportunities for green and cost-effective energy within the framework of the circular economy.

Acknowledgements

S.A.M. acknowledges a Phd scholarship on Green Issues from action IV.5 of the PON Research and Innovation 2014-2020 "Education and research for recovery – REACT- EU" program. C.F. acknowledges financial support from the Fondazione Cariplo through the grant “Cathode Recovery for Lithium Ion Battery Recycling – COLIBRI”. C.S. would like to thank the support from the Italian Ministry of Education, Universities and Research (Ministero dell’Istruzione, dell’Università e della Ricerca – MIUR) through the “Rita Levi Montalcini 2018” fellowship (Grant number PGR18MAZLI). The authors also thank the Italian ministry MIUR for funding through the FISR 2019 project AMPERE (FISR2019_01294).

Reference

[1] N. Nitta, F. Wu, J.T. Lee, G. Yushin, Li-ion battery materials: present and future, Materials Today. 18 (2015) 252–264. https://doi.org/10.1016/j.mattod.2014.10.040.

[2] L.-F. Zhou, D. Yang, T. Du, H. Gong, W.-B. Luo, The Current Process for the Recycling of Spent Lithium Ion Batteries, Frontiers in Chemistry. 8 (2020). https://www.frontiersin.org/article/10.3389/fchem.2020.578044 (accessed April 24, 2022).

[3] X. Zhang, L. Li, E. Fan, Q. Xue, Y. Bian, F. Wu, R. Chen, Toward sustainable and systematic recycling of spent rechargeable batteries, Chem. Soc. Rev. 47 (2018) 7239–7302. https://doi.org/10.1039/C8CS00297E.

[4] C. Ferrara, R. Ruffo, E. Quartarone, P. Mustarelli, Circular Economy and the Fate of Lithium Batteries: Second Life and Recycling, Advanced Energy and Sustainability Research. 2 (2021) 2100047. https://doi.org/10.1002/aesr.202100047.

[5] Priorities for critical materials for a circular economy, EASAC – the European Academies' Science Advisory Council, Halle (Saale) Germany, 2016.
[6] A. Chitre, D. Freake, L. Lander, J. Edge, M.-M. Titirici, Towards a More Sustainable Lithium-Ion Battery Future: Recycling LIBs from Electric Vehicles, Batteries & Supercaps. 3 (2020) 1126–1136. https://doi.org/10.1002/batt.202000146.
[7] M. Azevedo, N. Campagnol, T. Hagenbruch, K. Hoffman, A. Lala, O. Ramsbottom, Lithium and cobalt – a tale of two commodities, Metals and Mining McKinsey & Company, 2018.
[8] J.J. Roy, B. Cao, S. Madhavi, A review on the recycling of spent lithium-ion batteries (LIBs) by the bioleaching approach, Chemosphere. 282 (2021) 130944. https://doi.org/10.1016/j.chemosphere.2021.130944.
[9] R. Golmohammadzadeh, F. Faraji, F. Rashchi, Recovery of lithium and cobalt from spent lithium ion batteries (LIBs) using organic acids as leaching reagents: A review, Resources, Conservation and Recycling. 136 (2018) 418–435. https://doi.org/10.1016/j.resconrec.2018.04.024.
[10] X. Zhang, Q. Xue, L. Li, E. Fan, F. Wu, R. Chen, Sustainable Recycling and Regeneration of Cathode Scraps from Industrial Production of Lithium-Ion Batteries, ACS Sustainable Chem. Eng. 4 (2016) 7041–7049. https://doi.org/10.1021/acssuschemeng.6b01948.
[11] B. Swain, Recovery and recycling of lithium: A review, Separation and Purification Technology. 172 (2017) 388–403. https://doi.org/10.1016/j.seppur.2016.08.031.
[12] K.M. Winslow, S.J. Laux, T.G. Townsend, A review on the growing concern and potential management strategies of waste lithium-ion batteries, Resources, Conservation and Recycling. 129 (2018) 263–277. https://doi.org/10.1016/j.resconrec.2017.11.001.
[13] M.T. Islam, U. Iyer-Raniga, Lithium-Ion Battery Recycling in the Circular Economy: A Review, Recycling. 7 (2022) 33. https://doi.org/10.3390/recycling7030033.
[14] R. Golmohammadzadeh, F. Faraji, B. Jong, C. Pozo-Gonzalo, P.C. Banerjee, Current challenges and future opportunities toward recycling of spent lithium-ion batteries, Renewable and Sustainable Energy Reviews. 159 (2022) 112202. https://doi.org/10.1016/j.rser.2022.112202.
[15] F. Duarte Castro, M. Vaccari, L. Cutaia, Valorization of resources from end-of-life lithium-ion batteries: A review, Critical Reviews in Environmental Science and Technology. 52 (2022) 2060–2103. https://doi.org/10.1080/10643389.2021.1874854.
[16] G. Harper, R. Sommerville, E. Kendrick, L. Driscoll, P. Slater, R. Stolkin, A. Walton, P. Christensen, O. Heidrich, S. Lambert, A. Abbott, K. Ryder, L. Gaines, P. Anderson, Recycling lithium-ion batteries from electric vehicles, Nature. 575 (2019) 75–86. https://doi.org/10.1038/s41586-019-1682-5.
[17] Y. Kotak, C. Marchante Fernández, L. Canals Casals, B.S. Kotak, D. Koch, C. Geisbauer, L. Trilla, A. Gómez-Núñez, H.-G. Schweiger, End of Electric Vehicle Batteries: Reuse vs. Recycle, Energies. 14 (2021) 2217. https://doi.org/10.3390/en14082217.
[18] X. Zeng, J. Li, N. Singh, Recycling of Spent Lithium-Ion Battery: A Critical Review, Critical Reviews in Environmental Science and Technology. 44 (2014) 1129–1165. https://doi.org/10.1080/10643389.2013.763578.
[19] K. Singh, F. (Sanaz) Razmjooei, J.-S. Yu, Active sites and factors influencing them for efficient oxygen reduction reaction in metal-N coordinated pyrolyzed and non-pyrolyzed catalysts: A review, J. Mater. Chem. A. 5 (2017). https://doi.org/10.1039/C7TA05222G.

[20] N. Ramaswamy, S. Mukerjee, Fundamental Mechanistic Understanding of Electrocatalysis of Oxygen Reduction on Pt and Non-Pt Surfaces: Acid versus Alkaline Media, Advances in Physical Chemistry. 2012 (2012) e491604. https://doi.org/10.1155/2012/491604.
[21] M. Ďurovič, J. Hnát, K. Bouzek, Electrocatalysts for the hydrogen evolution reaction in alkaline and neutral media. A comparative review, Journal of Power Sources. 493 (2021) 229708. https://doi.org/10.1016/j.jpowsour.2021.229708.
[22] X. Zou, Y. Zhang, Noble metal-free hydrogen evolution catalysts for water splitting, Chem. Soc. Rev. 44 (2015) 5148–5180. https://doi.org/10.1039/C4CS00448E.
[23] F. Ullah, K. Ayub, T. Mahmood, High performance SACs for HER process using late first-row transition metals anchored on graphyne support: A DFT insight, International Journal of Hydrogen Energy. 46 (2021) 37814–37823. https://doi.org/10.1016/j.ijhydene.2021.09.063.
[24] X. Ge, A. Sumboja, D. Wuu, T. An, B. Li, F.W.T. Goh, T.S.A. Hor, Y. Zong, Z. Liu, Oxygen Reduction in Alkaline Media: From Mechanisms to Recent Advances of Catalysts, ACS Catal. 5 (2015) 4643–4667. https://doi.org/10.1021/acscatal.5b00524.
[25] Z. Liang, H. Zheng, R. Cao, Recent advances in Co-based electrocatalysts for the oxygen reduction reaction, Sustainable Energy Fuels. 4 (2020) 3848–3870. https://doi.org/10.1039/D0SE00271B.
[26] A. Badruzzaman, A. Yuda, A. Ashok, A. Kumar, Recent advances in cobalt based heterogeneous catalysts for oxygen evolution reaction, Inorganica Chimica Acta. 511 (2020) 119854. https://doi.org/10.1016/j.ica.2020.119854.
[27] W. Zhang, L. Cui, J. Liu, Recent advances in cobalt-based electrocatalysts for hydrogen and oxygen evolution reactions, Journal of Alloys and Compounds. 821 (2020) 153542. https://doi.org/10.1016/j.jallcom.2019.153542.
[28] H. Zhong, C.A. Campos-Roldán, Y. Zhao, S. Zhang, Y. Feng, N. Alonso-Vante, Recent Advances of Cobalt-Based Electrocatalysts for Oxygen Electrode Reactions and Hydrogen Evolution Reaction, Catalysts. 8 (2018) 559. https://doi.org/10.3390/catal8110559.
[29] X. Peng, X. Jin, B. Gao, Z. Liu, P.K. Chu, Strategies to improve cobalt-based electrocatalysts for electrochemical water splitting, Journal of Catalysis. 398 (2021) 54–66. https://doi.org/10.1016/j.jcat.2021.04.003.
[30] Q. Wang, R. Guo, Z. Wang, D. Shen, R. Yu, K. Luo, C. Wu, S. Gu, Progress in carbon-based electrocatalyst derived from biomass for the hydrogen evolution reaction, Fuel. 293 (2021) 120440. https://doi.org/10.1016/j.fuel.2021.120440.
[31] M. Muhyuddin, P. Mustarelli, C. Santoro, Recent Advances in Waste Plastic Transformation into Valuable Platinum-Group Metal-Free Electrocatalysts for Oxygen Reduction Reaction, ChemSusChem. 14 (2021) 3785–3800. https://doi.org/10.1002/cssc.202101252.
[32] M. Muhyuddin, J. Filippi, L. Zoia, S. Bonizzoni, R. Lorenzi, E. Berretti, L. Capozzoli, M. Bellini, C. Ferrara, A. Lavacchi, C. Santoro, Waste Face Surgical Mask Transformation into Crude Oil and Nanostructured Electrocatalysts for Fuel Cells and Electrolyzers, ChemSusChem. 15 (2022) e202102351. https://doi.org/10.1002/cssc.202102351.
[33] M. Borghei, J. Lehtonen, L. Liu, O.J. Rojas, Advanced Biomass-Derived Electrocatalysts for the Oxygen Reduction Reaction, Advanced Materials. 30 (2018) 1703691. https://doi.org/10.1002/adma.201703691.

[34] N. Prabu, R.S.A. Saravanan, T. Kesavan, G. Maduraiveeran, M. Sasidharan, An efficient palm waste derived hierarchical porous carbon for electrocatalytic hydrogen evolution reaction, Carbon. 152 (2019) 188–197. https://doi.org/10.1016/j.carbon.2019.06.016.
[35] Z. Chen, W. Wei, H. Chen, B.-J. Ni, Eco-designed electrocatalysts for water splitting: A path toward carbon neutrality, International Journal of Hydrogen Energy. (2022). https://doi.org/10.1016/j.ijhydene.2022.03.046.
[36] S. Li, S.-H. Ho, T. Hua, Q. Zhou, F. Li, J. Tang, Sustainable biochar as an electrocatalysts for the oxygen reduction reaction in microbial fuel cells, Green Energy & Environment. 6 (2021) 644–659. https://doi.org/10.1016/j.gee.2020.11.010.
[37] G. Daniel, T. Kosmala, M.C. Dalconi, L. Nodari, D. Badocco, P. Pastore, A. Lorenzetti, G. Granozzi, C. Durante, Upcycling of polyurethane into iron-nitrogen-carbon electrocatalysts active for oxygen reduction reaction, Electrochimica Acta. 362 (2020) 137200. https://doi.org/10.1016/j.electacta.2020.137200.
[38] S. Zago, M. Bartoli, M. Muhyuddin, G.M. Vanacore, P. Jagdale, A. Tagliaferro, C. Santoro, S. Specchia, Engineered biochar derived from pyrolyzed waste tea as a carbon support for Fe-N-C electrocatalysts for the oxygen reduction reaction, Electrochimica Acta. 412 (2022) 140128. https://doi.org/10.1016/j.electacta.2022.140128.
[39] H. Lv, H. Huang, C. Huang, Q. Gao, Z. Yang, W. Zhang, Electric field driven de-lithiation: A strategy towards comprehensive and efficient recycling of electrode materials from spent lithium ion batteries, Applied Catalysis B: Environmental. 283 (2021) 119634. https://doi.org/10.1016/j.apcatb.2020.119634.
[40] S. Wang, ning chen, J. Qi, X. Du, Y. Wang, W. Zhang, Y. Wang, Y. Lu, Recycled LiCoO2 in Spent Lithium-ion Battery as An Oxygen Evolution Electrocatalyst, RSC Adv. 6 (2016). https://doi.org/10.1039/C6RA23483F.
[41] J. Wei, S. Zhao, L. Ji, T. Zhou, Y. Miao, K. Scott, D. Li, J. Yang, X. Wu, Reuse of Ni-Co-Mn oxides from spent Li-ion batteries to prepare bifunctional air electrodes, Resources, Conservation and Recycling. 129 (2018) 135–142. https://doi.org/10.1016/j.resconrec.2017.10.021.
[42] V.C.B. Pegoretti, P.V.M. Dixini, L. Magnago, A.K.S. Rocha, M.F.F. Lelis, M.B.J.G. Freitas, High-temperature (HT) LiCoO2 recycled from spent lithium ion batteries as catalyst for oxygen evolution reaction, Materials Research Bulletin. 110 (2019) 97–101. https://doi.org/10.1016/j.materresbull.2018.10.022.
[43] T. Maiyalagan, K.A. Jarvis, S. Therese, P.J. Ferreira, A. Manthiram, Spinel-type lithium cobalt oxide as a bifunctional electrocatalyst for the oxygen evolution and oxygen reduction reactions, Nat Commun. 5 (2014) 3949. https://doi.org/10.1038/ncomms4949.
[44] T. Liu, S. Cai, G. Zhao, Z. Gao, S. Liu, H. Li, L. Chen, M. Li, X. Yang, H. Guo, Recycling valuable cobalt from spent lithium ion batteries for controllably designing a novel sea-urchin-like cobalt nitride-graphene hybrid catalyst: Towards efficient overall water splitting, Journal of Energy Chemistry. 62 (2021) 440–450. https://doi.org/10.1016/j.jechem.2021.03.052.
[45] R. Tao, P. Xing, H. Li, Z. Sun, Y. Wu, Recovery of spent LiCoO2 lithium-ion battery via environmentally friendly pyrolysis and hydrometallurgical leaching, Resources, Conservation and Recycling. 176 (2022) 105921. https://doi.org/10.1016/j.resconrec.2021.105921.

[46] Y. Shi, G. Chen, Z. Chen, Effective regeneration of LiCoO2 from spent lithium-ion batteries: a direct approach towards high-performance active particles, Green Chem. 20 (2018) 851–862. https://doi.org/10.1039/C7GC02831H.
[47] S. Zhou, Y. Zhang, Q. Meng, P. Dong, Z. Fei, Q. Li, Recycling of LiCoO2 cathode material from spent lithium ion batteries by ultrasonic enhanced leaching and one-step regeneration, Journal of Environmental Management. 277 (2021) 111426. https://doi.org/10.1016/j.jenvman.2020.111426.
[48] S. He, B.P. Wilson, M. Lundström, Z. Liu, Clean and efficient recovery of spent LiCoO2 cathode material: Water-leaching characteristics and low-temperature ammonium sulfate calcination mechanisms, Journal of Cleaner Production. 268 (2020) 122299. https://doi.org/10.1016/j.jclepro.2020.122299.
[49] A. Pražanová, V. Knap, D.-I. Stroe, Literature Review, Recycling of Lithium-Ion Batteries from Electric Vehicles, Part I: Recycling Technology, Energies. 15 (2022) 1086. https://doi.org/10.3390/en15031086.
[50] K.K. Jena, A. AlFantazi, A.T. Mayyas, Comprehensive Review on Concept and Recycling Evolution of Lithium-Ion Batteries (LIBs), Energy Fuels. 35 (2021) 18257–18284. https://doi.org/10.1021/acs.energyfuels.1c02489.
[51] M. Jafari, S.Z. Shafaie, H. Abdollahi, A. Entezari-Zarandi, A Green Approach for Selective Ionometallurgical Separation of Lithium from Spent Li-Ion Batteries by Deep Eutectic Solvent (DES): Process Optimization and Kinetics Modeling, Mineral Processing and Extractive Metallurgy Review. 0 (2022) 1–13. https://doi.org/10.1080/08827508.2022.2042282.
[52] S. Wang, Z. Zhang, Z. Lu, Z. Xu, A novel method for screening deep eutectic solvent to recycle the cathode of Li-ion batteries, Green Chem. 22 (2020) 4473–4482. https://doi.org/10.1039/D0GC00701C.
[53] C. Padwal, H.D. Pham, S. Jadhav, T.T. Do, J. Nerkar, L.T.M. Hoang, A. Kumar Nanjundan, S.G. Mundree, D.P. Dubal, Deep Eutectic Solvents: Green Approach for Cathode Recycling of Li-Ion Batteries, Advanced Energy and Sustainability Research. 3 (2022) 2100133. https://doi.org/10.1002/aesr.202100133.
[54] N. Peeters, K. Binnemans, S. Riaño, Solvometallurgical recovery of cobalt from lithium-ion battery cathode materials using deep-eutectic solvents, Green Chem. 22 (2020) 4210–4221. https://doi.org/10.1039/D0GC00940G.
[55] D.J. Miller, M.C. Biesinger, N.S. McIntyre, Interactions of CO2 and CO at fractional atmosphere pressures with iron and iron oxide surfaces: one possible mechanism for surface contamination?, Surface and Interface Analysis. 33 (2002) 299–305. https://doi.org/10.1002/sia.1188.
[56] W. Giurlani, M. Innocenti, A. Lavacchi, X-ray Microanalysis of Precious Metal Thin Films: Thickness and Composition Determination, Coatings. 8 (2018) 84. https://doi.org/10.3390/coatings8020084.
[57] W. Giurlani, E. Berretti, M. Innocenti, A. Lavacchi, Measuring the Thickness of Metal Coatings: A Review of the Methods, Coatings. 10 (2020) 1211. https://doi.org/10.3390/coatings10121211.
[58] Separation of nickel from cobalt and manganese in lithium ion batteries using deep eutectic solvents, Green Chemistry. 24 (2022) 4877–4886. https://doi.org/10.1039/d2gc00606e.

[59] F. Wang, R. Sun, J. Xu, Z. Chen, M. Kang, Recovery of cobalt from spent lithium ion batteries using sulphuric acid leaching followed by solid–liquid separation and solvent extraction, RSC Adv. 6 (2016) 85303–85311. https://doi.org/10.1039/C6RA16801A.
[60] Y. Shen, Recycling cathode materials of spent lithium-ion batteries for advanced catalysts production, Journal of Power Sources. 528 (2022) 231220. https://doi.org/10.1016/j.jpowsour.2022.231220.
[61] K. Feng, M. Li, W. Liu, A.G. Kashkooli, X. Xiao, M. Cai, Z. Chen, Silicon-Based Anodes for Lithium-Ion Batteries: From Fundamentals to Practical Applications, Small. 14 (2018) 1702737. https://doi.org/10.1002/smll.201702737.
[62] G.G. Eshetu, E. Figgemeier, Confronting the Challenges of Next-Generation Silicon Anode-Based Lithium-Ion Batteries: Role of Designer Electrolyte Additives and Polymeric Binders, ChemSusChem. 12 (2019) 2515–2539. https://doi.org/10.1002/cssc.201900209.
[63] A. Sarkar, R. May, S. Ramesh, W. Chang, L.E. Marbella, Recovery and Reuse of Composite Cathode Binder in Lithium Ion Batteries, ChemistryOpen. 10 (2021) 545–552. https://doi.org/10.1002/open.202100060.
[64] E. Zhen, J. Jiang, C. Lv, X. Huang, H. Xu, H. Dou, X. Zhang, Effects of binder content on low-cost solvent-free electrodes made by dry-spraying manufacturing for lithium-ion batteries, Journal of Power Sources. 515 (2021) 230644. https://doi.org/10.1016/j.jpowsour.2021.230644.
[65] A. Arif, M. Xu, J. Rashid, C.S. Saraj, W. Li, B. Akram, B. Hu, Efficient Recovery of Lithium Cobaltate from Spent Lithium-Ion Batteries for Oxygen Evolution Reaction, Nanomaterials. 11 (2021) 3343. https://doi.org/10.3390/nano11123343.
[66] M. Zhou, F. Lu, X. Shen, W. Xia, H. He, X. Zeng, One-pot Construction of Three Dimensional CoMoO4/Co3O4 Hybrid Nanostructures and Their Application in Supercapacitors, J. Mater. Chem. A. 3 (2015). https://doi.org/10.1039/C5TA05658F.
[67] M. Fang, W.-B. Xu, S. Han, P. Cao, W. Xu, D. Zhu, Y. Lu, W. Liu, Enhanced urea oxidization electrocatalysis on spinel cobalt oxide nanowires via on-site electrochemical defect engineering, Mater. Chem. Front. 5 (2021) 3717–3724. https://doi.org/10.1039/D0QM01119C.
[68] Q. Liang, H. Yue, W. Zhou, Q. Wei, Q. Ru, Y. Huang, H. Lou, F. Chen, X. Hou, Structure Recovery and Recycling of Used LiCoO2 Cathode Material, Chemistry – A European Journal. 27 (2021) 14225–14233. https://doi.org/10.1002/chem.202102015.
[69] M.C. Biesinger, B.P. Payne, A.P. Grosvenor, L.W.M. Lau, A.R. Gerson, R.St.C. Smart, Resolving surface chemical states in XPS analysis of first row transition metals, oxides and hydroxides: Cr, Mn, Fe, Co and Ni, Applied Surface Science. 257 (2011) 2717–2730. https://doi.org/10.1016/j.apsusc.2010.10.051.
[70] Z.-W. Fu, C.-L. Li, W.-Y. Liu, J. Ma, Y. Wang, Q.-Z. Qin, Electrochemical Reaction of Lithium with Cobalt Fluoride Thin Film Electrode, J. Electrochem. Soc. 152 (2004) E50. https://doi.org/10.1149/1.1839512.
[71] M. Mandal, Recent Advancement on Anion Exchange Membranes for Fuel Cell and Water Electrolysis, ChemElectroChem. 8 (2021) 36–45. https://doi.org/10.1002/celc.202001329.
[72] C. Santoro, A. Lavacchi, P. Mustarelli, V. Di Noto, L. Elbaz, D.R. Dekel, F. Jaouen, What is Next in Anion-Exchange Membrane Water Electrolyzers? Bottlenecks, Benefits, and Future, ChemSusChem. 15 (2022) e202200027. https://doi.org/10.1002/cssc.202200027.

[73] W. Moschkowitsch, O. Lori, L. Elbaz, Recent Progress and Viability of PGM-Free Catalysts for Hydrogen Evolution Reaction and Hydrogen Oxidation Reaction, ACS Catal. 12 (2022) 1082–1089. https://doi.org/10.1021/acscatal.1c04948.
[74] O. Lori, N. Zion, H.C. Honig, L. Elbaz, 3D Metal Carbide Aerogel Network as a Stable Catalyst for the Hydrogen Evolution Reaction, ACS Catal. 11 (2021) 13707–13713. https://doi.org/10.1021/acscatal.1c03332.
[75] H. Jin, J. Wang, D. Su, Z. Wei, Z. Pang, Y. Wang, In situ Cobalt–Cobalt Oxide/N-Doped Carbon Hybrids As Superior Bifunctional Electrocatalysts for Hydrogen and Oxygen Evolution, J. Am. Chem. Soc. 137 (2015) 2688–2694. https://doi.org/10.1021/ja5127165.
[76] S.C. Petitto, E.M. Marsh, G.A. Carson, M.A. Langell, Cobalt oxide surface chemistry: The interaction of CoO(100), Co3O4(110) and Co3O4(111) with oxygen and water, Journal of Molecular Catalysis A: Chemical. 281 (2008) 49–58. https://doi.org/10.1016/j.molcata.2007.08.023.
[77] T. Zhang, Y. Sun, L. Hang, Y. Bai, X. Li, L. Wen, X. Zhang, X. Lyu, W. Cai, Y. Li, Large-Scale Synthesis of Co/CoOx Encapsulated in Nitrogen-, Oxygen-, and Sulfur-Tridoped Three-Dimensional Porous Carbon as Efficient Electrocatalysts for Hydrogen Evolution Reaction, ACS Applied Energy Materials. 1 (2018) 6250–6259. https://doi.org/10.1021/acsaem.8b01272.
[78] P. Guo, J. Wu, X.-B. Li, J. Luo, W.-M. Lau, H. Liu, X.-L. Sun, L.-M. Liu, A highly stable bifunctional catalyst based on 3D Co(OH)2@NCNTs@NF towards overall water-splitting, Nano Energy. 47 (2018) 96–104. https://doi.org/10.1016/j.nanoen.2018.02.032.
[79] T.-W. Chiou, I.-J. Hsu, W.-L. Li, C.-Y. Tung, Z.-Q. Yang, J.-F. Lee, T.-W. Lin, Fluoride-incorporated cobalt-based electrocatalyst towards enhanced hydrogen evolution reaction, Chem. Commun. 58 (2022) 2746–2749. https://doi.org/10.1039/D1CC05375B.
[80] S. Rojas-Carbonell, C. Santoro, A. Serov, P. Atanassov, Transition metal-nitrogen-carbon catalysts for oxygen reduction reaction in neutral electrolyte, Electrochemistry Communications. 75 (2017) 38–42. https://doi.org/10.1016/j.elecom.2016.12.011.
[81] C. Santoro, M. Kodali, S. Herrera, A. Serov, I. Ieropoulos, P. Atanassov, Power generation in microbial fuel cells using platinum group metal-free cathode catalyst: Effect of the catalyst loading on performance and costs, Journal of Power Sources. 378 (2018) 169–175. https://doi.org/10.1016/j.jpowsour.2017.12.017.
[82] A. Bonakdarpour, M. lefèvre, R. Yang, F. Jaouen, T. Dahn, J.-P. Dodelet, J. Dahn, Impact of Loading in RRDE Experiments on Fe-N-C Catalysts: Two- or Four-Electron Oxygen Reduction?, Electrochemical and Solid State Letters. 11 (2008) B105–B108. https://doi.org/10.1149/1.2904768.
[83] M. Muhyuddin, N. Zocche, R. Lorenzi, C. Ferrara, F. Poli, F. Soavi, C. Santoro, Valorization of the inedible pistachio shells into nanoscale transition metal and nitrogen codoped carbon-based electrocatalysts for hydrogen evolution reaction and oxygen reduction reaction, Mater Renew Sustain Energy. 11 (2022) 131–141. https://doi.org/10.1007/s40243-022-00212-5.
[84] M. Muhyuddin, D. Testa, R. Lorenzi, G.M. Vanacore, F. Poli, F. Soavi, S. Specchia, W. Giurlani, M. Innocenti, L. Rosi, C. Santoro, Iron-based electrocatalysts derived from scrap tires for oxygen reduction reaction: Evolution of synthesis-structure-performance relationship in acidic, neutral and alkaline media, Electrochimica Acta. 433 (2022) 141254. https://doi.org/10.1016/j.electacta.2022.141254.

[85] T.J. Bandosz, Revealing the impact of small pores on oxygen reduction on carbon electrocatalysts: A journey through recent findings, Carbon. 188 (2022) 289–304. https://doi.org/10.1016/j.carbon.2021.11.071.
[86] O. Klepel, S. Utgenannt, C. Vormelchert, M. König, A. Meißner, F. Hansen, J.-H. Bölte, T. Sieber, R. Heinemann, M. Bron, A. Rokicińska, S. Jarczewski, P. Kuśtrowski, Redox catalysts based on amorphous porous carbons, Microporous and Mesoporous Materials. 323 (2021) 111257. https://doi.org/10.1016/j.micromeso.2021.111257.
[87] X. Huang, T. Shen, T. Zhang, H. Qiu, X. Gu, Z. Ali, Y. Hou, Efficient Oxygen Reduction Catalysts of Porous Carbon Nanostructures Decorated with Transition Metal Species, Advanced Energy Materials. 10 (2020) 1900375. https://doi.org/10.1002/aenm.201900375.
[88] X. Zhao, X. Zou, X. Yan, C.L. Brown, Z. Chen, G. Zhu, X. Yao, Defect-driven oxygen reduction reaction (ORR) of carbon without any element doping, Inorg. Chem. Front. 3 (2016) 417–421. https://doi.org/10.1039/C5QI00236B.
[89] M. Muhyuddin, A. Friedman, F. Poli, E. Petri, H. Honig, F. Basile, A. Fasolini, R. Lorenzi, E. Berretti, M. Bellini, A. Lavacchi, L. Elbaz, C. Santoro, F. Soavi, Lignin-derived bimetallic platinum group metal-free oxygen reduction reaction electrocatalysts for acid and alkaline fuel cells, Journal of Power Sources. 556 (2023) 232416. https://doi.org/10.1016/j.jpowsour.2022.232416.
[90] J. Liu, L. Jiang, B. Zhang, J. Jin, D.S. Su, S. Wang, G. Sun, Controllable Synthesis of Cobalt Monoxide Nanoparticles and the Size-Dependent Activity for Oxygen Reduction Reaction, ACS Catal. 4 (2014) 2998–3001. https://doi.org/10.1021/cs500741s.
[91] Y. Liang, Y. Li, H. Wang, J. Zhou, J. Wang, T. Regier, H. Dai, Co3O4 nanocrystals on graphene as a synergistic catalyst for oxygen reduction reaction, Nature Mater. 10 (2011) 780–786. https://doi.org/10.1038/nmat3087.
[92] Z.-J. Jiang, Z. Jiang, Interaction Induced High Catalytic Activities of CoO Nanoparticles Grown on Nitrogen-Doped Hollow Graphene Microspheres for Oxygen Reduction and Evolution Reactions, Sci Rep. 6 (2016) 27081. https://doi.org/10.1038/srep27081.
[93] S. Liang, Q. An, S. Wang, Z. Chen, L. Huang, L. Zhao, Sub-3 nm CoO Nanoparticles with Oxygen Vacancy-Dependent Catalytic Activity for the Oxygen Reduction Reaction, ACS Appl. Nano Mater. 5 (2022) 8214–8223. https://doi.org/10.1021/acsanm.2c01296.
[94] J. Wang, R. Gao, D. Zhou, Z. Chen, Z. Wu, G. Schumacher, Z. Hu, X. Liu, Boosting the Electrocatalytic Activity of Co3O4 Nanosheets for a Li-O2 Battery through Modulating Inner Oxygen Vacancy and Exterior Co3+/Co2+ Ratio, ACS Catal. 7 (2017) 6533–6541. https://doi.org/10.1021/acscatal.7b02313.
[95] G. Jia, F. Li, J. Wang, S. Liu, Y. Yang, Dual Substitution Strategy in Co-Free Layered Cathode Materials for Superior Lithium Ion Batteries, ACS Appl. Mater. Interfaces. 13 (2021) 18733–18742. https://doi.org/10.1021/acsami.1c01221.
[96] S. Lee, A. Manthiram, Can Cobalt Be Eliminated from Lithium-Ion Batteries?, ACS Energy Lett. 7 (2022) 3058–3063. https://doi.org/10.1021/acsenergylett.2c01553.
[97] A. Hebert, E. McCalla, The role of metal substitutions in the development of Li batteries, part I: cathodes, Mater. Adv. 2 (2021) 3474–3518. https://doi.org/10.1039/D1MA00081K.
[98] S.W.D. Gourley, T. Or, Z. Chen, Breaking Free from Cobalt Reliance in Lithium-Ion Batteries, IScience. 23 (2020) 101505. https://doi.org/10.1016/j.isci.2020.101505.